

High-sensitive terahertz detection by parametric up-conversion using nanosecond pulsed laser

Yuye Wang(王与烨), Gang Nie(聂港), Changhao Hu(胡常灏), Kai Chen(陈锴), Chao Yan(闫超), Bin Wu(吴斌), Junfeng Zhu(朱军峰), Degang Xu(徐德刚), and Jianquan Yao(姚建铨)

Citation: Chin. Phys. B, 2022, 31 (**2**): 024204. DOI: 10.1088/1674-1056/ac2d20
Journal homepage: http://cpb.iphy.ac.cn; http://iopscience.iop.org/cpb

What follows is a list of articles you may be interested in

Efficient manipulation of terahertz waves by multi-bit coding metasurfaces and further applications of such metasurfaces

Yunping Qi(祁云平) Baohe Zhang(张宝和), Jinghui Ding(丁京徽), Ting Zhang(张婷), Xiangxian Wang(王向贤), and Zao Yi(易早)
Chin. Phys. B, 2021, 30 (**2**): 024211. DOI: 10.1088/1674-1056/abd6fc

Theoretical research on terahertz wave generation from planar waveguide by optimized cascaded difference frequency generation

Zhongyang Li(李忠洋), Jia Zhao(赵佳), Wenkai Liu(刘文锴), Qingfeng Hu(胡青峰), Yongjun Li(李永军), Binzhe Jiao(焦彬哲), Pibin Bing(邴丕彬), Hongtao Zhang(张红涛), Lian Tan(谭联), and Jianquan Yao(姚建铨)
Chin. Phys. B, 2021, 30 (**2**): 024209. DOI: 10.1088/1674-1056/abc3b7

Multi-functional vanadium dioxide integrated metamaterial for terahertz wave manipulation

Jian-Xing Zhao(赵建行), Jian-Lin Song(宋建林), Yao Zhou(周姚), Rui-Long Zhao(赵瑞龙), Yi-Chao Liu(刘艺超), Jian-Hong Zhou(周见红)
Chin. Phys. B, 2020, 29 (**9**): 094205. DOI: 10.1088/1674-1056/abab6f

Active metasurfaces for manipulatable terahertz technology

Jing-Yuan Wu(吴静远), Xiao-Feng Xu(徐晓峰), Lian-Fu Wei(韦联福)
Chin. Phys. B, 2020, 29 (**9**): 094202. DOI: 10.1088/1674-1056/aba613

Pancharatnam-Berry metasurface for terahertz wave radar cross section reduction

Shao-He Li(李绍和), Jiu-Sheng Li(李九生)
Chin. Phys. B, 2019, 28 (**9**): 094210. DOI: 10.1088/1674-1056/ab33f5

High-sensitive terahertz detection by parametric up-conversion using nanosecond pulsed laser

Yuye Wang(王与烨)[1,2], Gang Nie(聂港)[1,2], Changhao Hu(胡常灏)[1,2], Kai Chen(陈锴)[1,2], Chao Yan(闫超)[1,2], Bin Wu(吴斌)[3], Junfeng Zhu(朱军峰)[3], Degang Xu(徐德刚)[1,2,†], and Jianquan Yao(姚建铨)[1,2]

[1] *Institute of Laser and Optoelectronics, School of Precision Instruments and Optoelectronics Engineering, Tianjin University, Tianjin* 300072, *China*

[2] *Key Laboratory of Optoelectronic Information Technology (Ministry of Education), Tianjin University, Tianjin* 300072, *China*

[3] *Science and Technology on Electronic Test & Measurement Laboratory, Qingdao* 266555, *China*

(Received 18 August 2021; revised manuscript received 16 September 2021; accepted manuscript online 6 October 2021)

A high-sensitive terahertz detector operating at room temperature was demonstrated based on parametric up-conversion. A nanosecond 1064-nm Nd:YAG laser was used to pump the parametric up-conversion detector and the up-conversion from terahertz wave to NIR laser was realized in a lithium niobate crystal. The minimum detectable terahertz energy of 9 pJ was realized with the detection dynamic range of 54 dB, which was three orders of magnitude higher than that of commercial Golay cell. The detectable terahertz frequency range of the detection system was 0.90 Thz–1.83 THz. Besides, the effects of pump energy and effective gain length on the detection sensitivity were studied in experiment. The results showed that higher pump energy and longer effective gain length are helpful for improving the detection sensitivity of parametric up-conversion detector.

Keywords: terahertz wave, high-sensitive detection, room temperature operation, parametric up-conversion

PACS: 42.65.Dr, 87.50.U–, 42.65.–k, 42.60.–v **DOI:** 10.1088/1674-1056/ac2d20

1. Introduction

Terahertz wave (THz wave) lies between the microwave and infrared regions in the electromagnetic spectrum. Due to the unique properties, THz wave has received much attention in several areas, such as 6G communication technology, biomedicine, security and spectrum detection.[1–4] With the development of THz technologies in these applications, the highly sensitive, room-temperature THz detector has become a hot spot.

At present, the commonly used THz wave detectors mainly include cryogenically cooled (4.2 K) Si bolometer, Golay cell and pyroelectric detector and electro-optical sampling. Though Si bolometer has high detection sensitivity, it must be operated at 4.2 K cryogenic temperatures cooled by liquid helium. Besides, due to the rapid evaporation of liquid helium, it is typically operated continuously for a few days at a time. Both Golay cell and pyroelectric detector are based on the thermal response of detection materials in THz band. Although they are able to operate at room temperature, they have the disadvantages of long response time and low detection sensitivity. Especially, these detectors are vulnerable to the interference of ambient temperature and vibration. Electro-optical sampling is a widely used method of terahertz time domain detection. It has the characteristic of high sensitivity in wide THz range. However, a femtosecond pump laser is necessary to achieve sensitive THz detection, which increases the system cost.[5–7] Based on the stimulated polariton scattering and optical parametric amplification in nonlinear crystals, parametric up-conversion detection has been demonstrated as a promising THz detector for possessing the advantages of widely detectable range, high sensitivity, fast response, and room temperature operation.[8–10] Through the input of THz wave and intense laser in nonlinear crystal simultaneously, the THz wave with low energy could be up-converted to be near infrared Stokes laser under the non-collinear phase-matching condition. Thus, THz wave can be indirectly measured by using the high-sensitive near-infrared detector.

For THz parametric detector, $LiNbO_3$ (LN) crystal is the most commonly used THz parametric up-conversion gain crystal, which has the advantages of high second- and third-order non-linearity coefficients. Sub-nanosecond (ns) laser and ns laser have been employed as the pump sources for the parametric up-conversion detection. Considering sub-ns laser can suppress the stimulated Brillouin scattering (SBS) in $LiNbO_3$ crystal effectively, it can improve the conversion efficiency of stimulated polariton scattering[11–14] and furtherly enhance the detection sensitivity of THz parametric up-conversion detection.[15–17] Until now, the highest detection sensitivity of THz wave has reached to 130 zJ by using two LN crystals, where the latter one was utilized to enhance the parametric amplification process, and the THz detection range of 0.6 THz–2.0 THz was realized.[18] Moreover, the THz-wave radiation from continuous-wave (CW) resonant tunneling diodes (RTDs) at 0.58, 0.78, and 1.14 THz was de-

[†]Corresponding author. E-mail: xudegang@tju.edu.cn

© 2022 Chinese Physical Society and IOP Publishing Ltd

tected using the parametric up-conversion detector. The minimum detection limit was as low as 5 nW at 1.14 THz.[19,20] Compared with sub-ns laser, ns laser has the advantages of high pulse energy, low price, and simple construction. It has been used for the widely tunable, high energy THz generation based on stimulated polariton scattering.[21–23] Therefore, ns laser has a good prospect in the field of THz parametric up-conversion detection. In 2008, Guo *et al.* realized THz parametric up-conversion detector pumped by ns 1064-nm laser firstly. The sensitive THz wave detection was realized at a single frequency by using fast response InGaAs detector to detect up-converted signal.[24] Then, they developed an automatic achromatic THz parametric up-conversion detection system, where the detection of a wide frequency range of 1.26 THz–2.63 THz was realized. The minimum detectable THz energy was 0.1 pJ at the frequency of 1.5 THz with the dynamic range of 20 dB.[25] Especially, to date there has been no detailed study on experiment of the impact factors for the THz parametric up-conversion detection sensitivity using ns laser pump.

In this paper, we present a high-sensitive THz parametric up-conversion detector pumped by a ns 1064-nm Nd:YAG laser. The THz wave in the frequency range of 0.90 THz–1.83 THz was detected with high sensitivity. The minimum detectable THz wave energy at 1.45 THz was 9 pJ and the dynamic range was 54 dB. Moreover, the effects of pump energy and effective gain length on the detection sensitivity of parametric up-conversion detector were studied experimentally.

2. Experimental setup

Figure 1 shows the schematic diagram of THz parametric up-conversion detection, which was mainly composed of THz wave parametric generator (TPG) and THz parametric up-conversion detector. The THz parametric generator and THz parametric up-conversion detector were pumped by a multimode Q-switched 1064-nm ns laser with repetition rate of 10 Hz and pulse-width of 10 ns. The 1064-nm laser with the beam diameter of 4 mm was divided into three beams by the mirrors M_1 and M_7 in sequence. One beam was frequency doubled to generate 532-nm laser, which was used to generate pulse seed laser. The other two beams were used as the pump beam of TPG and THz parametric up-conversion detector, which were named as pump No. 1 and pump No. 2 here, respectively. The THz gain medium of the TPG was a 1-mol.% magnesium oxide doped near-stoichiometric lithium niobate (MgO:SLN) crystal, which was cut as an isosceles trapezoid configuration. The longer base and the shorter base of the isosceles trapezoid were 40 mm and 23.2 mm, respectively. The thickness of the crystal along the z axis was 10 mm. The structure of THz parametric generator was similar to our pervious injection pulse-seeded THz-wave parametric generator (ips-TPG),[20] which can effectively improve the output energy of THz wave and expand its frequency tuning range because of the improvement on interaction of stimulated polariton scattering (SPS) and difference frequency generation (DFG) processes. The tunable pulse-seed laser from 1067 nm to 1076 nm was provided by a single resonant optical parametric oscillator (SR-OPO) pumped by 532-nm laser, consisted of two cavity mirrors M_3 and M_4, a KTP_2 crystal (10 mm $\times$8 mm $\times$20 mm, $\theta = 90°$, $\varphi = 24.5°$) and a Brewster polarizer (BP_1). Pump No. 1 and pulse-seed laser were injected into SLN crystal simultaneously, and the completely overlap of pump and pulse seed beams in the time domain was achieved by controlling the optical path of the pump beam. Different non-collinear phase-matching condition can be satisfied by rotating mirror M_6 and the continuously tunable THz wave with frequency of 0.8 THz–3 THz can be realized with the THz energy instability of 5.6%.[20] The THz wave generated by ips-TPG was nearly perpendicular to the longer base of SLN crystal, whose beam quality was not very good. Therefore, the THz wave should be shaped and focused before entering the THz parametric up-conversion detector to make sure the enough power density. An off-axis parabolic mirror OAP_1 shaped the THz wave into a parallel beam, and then the THz wave was focused by a TPX lens L_1. The size of the THz spot at the focus point was about 5mm at frequency of 1.45 THz. Furthermore, the THz energy was detected by a Golay cell (TYDEX, Inc.: GC-1P), which was covered by a 1-mm black polyethylene sheet to filter out the scattering infrared signals.

The gain mediums of the THz parametric up-conversion detector were a trapezoidal and a rectangular 5-mol.% magnesium oxide doped congruent lithium niobate (CLN_1 and CLN_2) crystals. The base angle of CLN_1 was 65°. The sizes of the two bases were 55 mm and 37.4 mm, respectively. The thickness of the crystal along the z axis was 10 mm. The size of the CLN_2 was 12 mm $\times$45 mm $\times$10 (z axis) mm. The z-axis direction of CLN_2 was parallel to the z axis direction of CLN_1. Besides, the y–z plane of CLN_2 was close to the side waist of the crystal CLN_1. The focus of THz wave and 1064-nm laser pump No. 2 were mixed at the base of crystal CLN_1. By rotating mirror M_{11}, different non-collinear phase-matching condition can be satisfied, so that the THz wave could be up-converted to an NIR beam (we call it the up-converted signal). The up-converted signal was generated and amplified in crystal CLN_1, and then entered into the rectangular crystal CLN_2 together with the residual pump beam. Because they met the phase matching condition, the up-converted signal can be further amplified in CLN_2. Careful attention must be paid to separate the up-converted signal and residual pump beam because the angle between them outside the crystal was small (about 1°–3°), which are easy to be mixed so that the measure of the

up-converted signal could be interfered. A D-shaped mirror M_{13} and a special coated mirror M_{14} were used to separate the up-converted signal and residual pump beam in space. Mirror M_{14} was coated with high transmission (more than 98%) in the 1063-nm to 1064.7-nm wavelength range and high reflection in the range of 1067 nm to 1078 nm ($R > 70\%$ at 1067 nm to 1070 nm, $R > 90\%$ at 1070 nm to 1078 nm) at the incident angle of 30°. By fine adjusting the angle of M_{14}, the up-converted signal could be totally reflected into the NIR detector, while the residual pump light was almost transmitted. In addition, an iris was used to block the broadband spontaneous signal generated by TPG and the residual weak pump beam. The wavelength and energy of up-converted signal was measured using an optical spectrometer (Avantes, Inc.: AVS-DESKTOP-USB2) and a fast response InGaAs detector (Thorlabs DET08C), respectively. The black polyethylene sheets with different thicknesses were used as attenuator to change the injected THz energy.

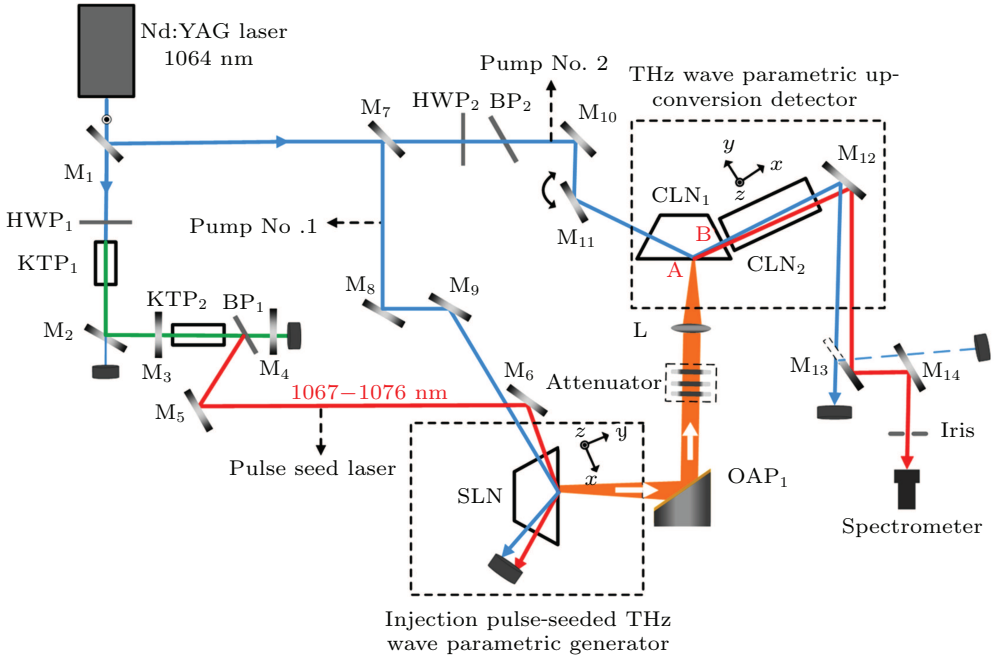


Fig. 1. Schematic diagram of THz parametric up-conversion detection.

3. Results and discussion

Considering the high absorption of THz wave in LN crystal (30 cm^{-1}@1.5 THz),[26] the injected THz energy would decrease to 10% after 0.8-mm transmission in LN. Thus, the pump No. 2 and injected THz wave just interacted around the surface of crystal CLN_1 in simplicity. In other words, the up-converted signal was firstly generated at the interacted area of pump No. 2 and THz wave in CLN_1 crystal, and then amplified in CLN_1 and CLN_2 along the optical path. Thus, the distance from the total reflection point of the pump beam No. 2 on the base of the crystal CLN_1 to the emission point (*i.e.*, line AB in Fig. 1), plus the length of the rectangular crystal CLN_2 was called as the effective gain length. When the effective gain length was 80 mm, and the energies of pump No. 2 and injected THz wave were 11 mJ and 2.5 μJ respectively, the wavelengths of the up-converted signal and Stokes laser generated from ips-TPG were measured, as shown in Fig. 2(a). The wavelengths of the up-converted signal and the Stokes laser were observed to be same (1069.63 nm), which indicates the accuracy of the parametric up-conversion detection for the measurement of THz frequency. Besides, it is clearly seen that the linewidth of the up-converted signal was much narrower than that of the corresponding Stokes laser. On one hand, the linewidth of Stokes laser generated from ips-TPG was relative wider compared with the traditional TPO system without the mode-selecting effect from cavity. The corresponded THz wave also had a certain linewidth according to the energy conservation equation $\omega_p = \omega_s + \omega_T$. On the other hand, THz energy at the center frequency was relatively high, it is dominant in the nonlinear frequency up-conversion. However, THz energy far from the center frequency was lower, and there was a larger phase mismatching with the pump beam. As a result, the efficiency of frequency up-conversion was low. Thus, the linewidth of the up-converted signal was narrowed for up-conversion detection. It should be mentioned that, the spontaneous parametric signal, whose wavelength and direction are same to that of up-converted signal, would be observed as the pump energy is high enough. In order to avoid the impact of spontaneous parametric signal, the pump energy was controlled in the experiment. Figure 2(b) shows the temporal profile of the up-converted signal measured by a high-speed InGaAs photodiode. The pulse width was 4.8-ns full-width at

the half maximum.

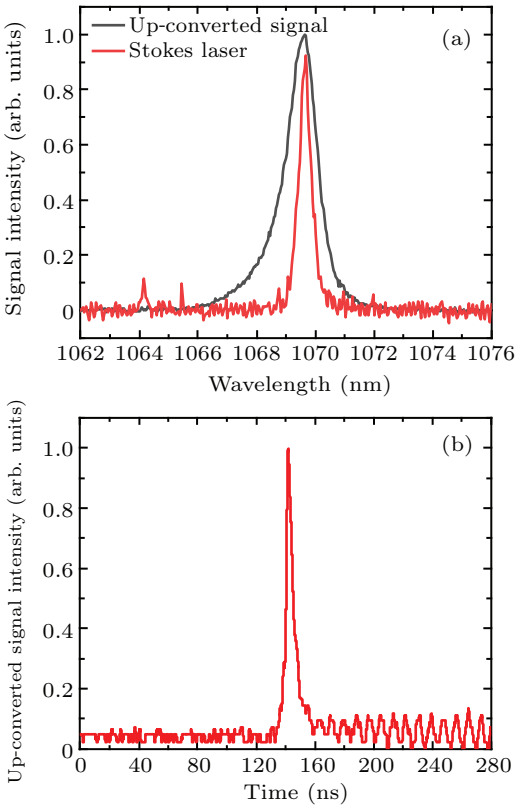


Fig. 2. (a) Up-converted signal and Stokes laser generated from ips-TPG measured by spectrometer. (b) The temporal profile of up-converted signal.

In order to determine the detection sensitivity of the THz parametric up-conversion detection system, we used five pieces of black polyethylene sheets with different thicknesses to attenuate the THz waves. The transmittances for five black polyethylene sheets were measured by a THz time-domain spectrometer (Advantest Corp., TAS7500SP). The different THz transmittance can be obtained by the combination of black polyethylene sheets of different thicknesses. Figure 3(a) shows the measured spectrum of up-converted signal with different THz attenuation under the pump energy of 11 mJ and the effective gain length of 80 mm, where the spontaneous parametric signal could not be measured by the spectrometer. The THz frequency was 1.45 THz, and the THz output energy of the THz parametric generator was 2.5 μJ. It is seen from Fig. 3(a) that, a clear spectral signal with wavelength of 1069.63 nm can be observed even when the THz energy was 9 pJ. Here, 9 pJ corresponded to the transmittance of 0.00036%, a combination of five black polyethylene sheets with transmittances of 56.7%, 34.7%, 5.36%, 3.74%, and 0.93% at 1.45 THz, respectively. Therefore, the minimum detectable THz energy was deduced to be 9 pJ with the dynamic range of 54 dB. Furthermore, THz wave under the attenuation of the above five black polyethylene sheets was measured by a 4-K-helium cooled Si bolometer, as shown in the inset of Fig. 3(a). The detected THz energy was 17 pJ, which was close to our results above (9 pJ). Therefore, it is believed that the detection sensitivity measured by parametric up-conversion is reliable. Additionally, 1064-nm pump could be observed in Fig. 3(a). However, compared to the up-converted signal, the energy of the residual 1064-nm pump was very low, which was neglected in our following experiment.

Figure 3(b) shows the readout voltage from InGaAs photodiode (*i.e.*, the up-converted signal voltage) as a function of the THz energy at 1.45 THz. In order to avoid the damage to the photodiode, the up-converted signal was attenuated using NIR coated mirrors with different transmittance. It is seen that, the higher the THz energy was, the larger the up-converted signal voltage was. Furthermore, the minimum detectable THz wave energies of Golay cell and bolometer were also measured through changing the attenuation sheets, which were 3.5 nJ and 0.6 pJ, respectively. The detection sensitivity of the parametric up-conversion detection method in our experiment is 3 orders of magnitude higher than that of Golay cell, but one order of magnitude lower than that of bolometer.

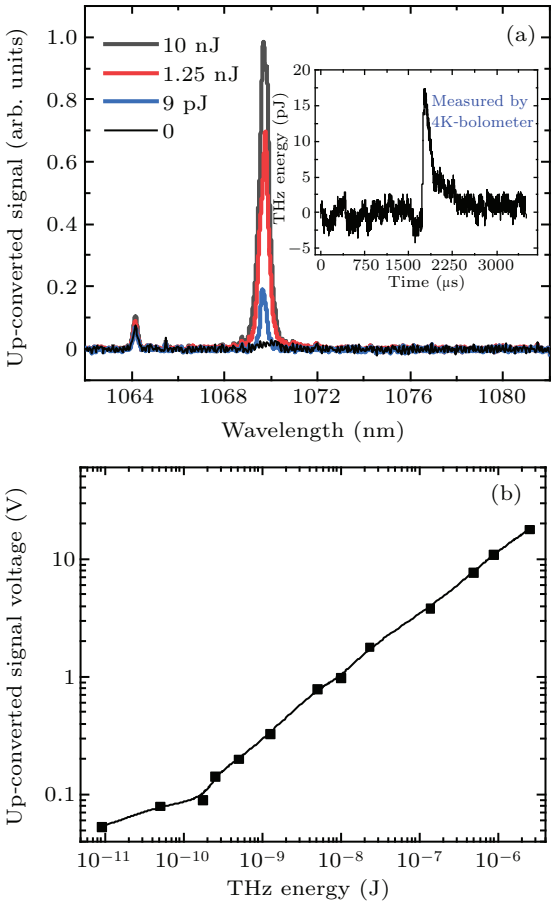


Fig. 3. (a) Measured spectrum of up-converted signal with different THz attenuation. Inset: the temporal profile of the up-converted signal measured by Si bolometer. (b) Readout voltage from InGaAs photodiode as a function of the THz energy.

Next, the effect of pump energy on the parametric up-conversion detection sensitivity was investigated. Figure 4(a) shows the readout up-converted signal voltage from InGaAs photodiode as a function of pump energy under different THz

energy. The pump threshold energies at THz energies of 2.5 μJ, 25 nJ, and 1.25 nJ was 2 mJ, 6 mJ, and 8 mJ, respectively. However, the threshold pump energy of spontaneous parametric noise without THz input was 11 mJ. With the pump energy increased from 2 mJ to 30 mJ, the intensity of up-converted signal gradually increased. Especially, the intensity of up-converted signal increased with the input THz energy under a certain pump energy. Although the spontaneous parametric noise was also increased with pump energy increasing, it was very low compared with the up-converted signal. In order not to be disturbed by spontaneous parametric signals, the pump energy of 11 mJ was chosen as upper limit, at which no spontaneous parametric signal was detected in the spectrometer. Figure 4(b) shows the minimum detectable THz energy as a function of pump energy for the parametric up-conversion detection. As the pump energy increased from 4 mJ to 11 mJ, the minimum detectable THz energy decreased from 2.5 μJ to 9 pJ. It means the detection sensitivity can be improved 6 orders of magnitude by improving the pump energy. Therefore, the pump energy should be chosen to be higher for the better detection sensitivity and avoid generating the spontaneous parametric noise at the same time.

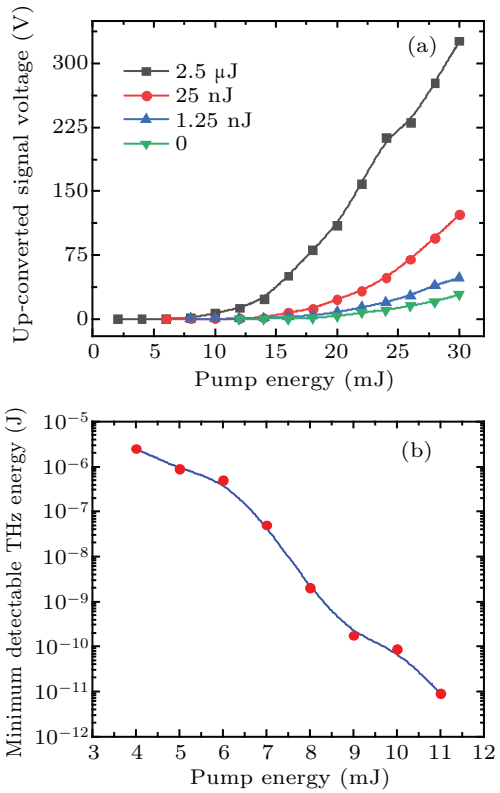


Fig. 4. (a) The readout voltage from InGaAs photodiode (*i.e.*, the up-converted signal voltage) as a function of pump energy. (b) The minimum detectable THz wave energy as a function of pump energy.

Figure 5(a) shows the measured voltage of the up-converted signal as a function of pump energy at different effective gain lengths. Through changing the incident point A of pump No. 2 on the surface of crystal CLN_1, the length of the AB section for up-converted signal can be changed simultaneously. Thus, the effective gain length of parametric up-conversion system is varied without changing the crystal. As the pump energy increased from 2 mJ to 30 mJ, the up-converted signal intensity increased gradually and were higher at longer effective gain length. In addition, the pump thresholds for the effective gain lengths of 70 mm, 80 mm, and 90 mm were 6 mJ, 4 mJ, and 2 mJ, respectively. Furthermore, we investigated the effect of effective gain length on the detection sensitivity, as shown in Fig. 5(b). When the effective gain lengths were 25 mm, 35 mm, and 45 mm, the experimental detection were performed without CLN_2 crystal. The pump energy was kept at 8 mJ, at which no spontaneous signal was generated for the maximum effective gain length of 90 mm. It is clearly that, the minimum detectable THz energy was reduced from 500 nJ to 9 pJ with the effective gain length increasing from 25 mm to 90 mm. Therefore, the longer effective gain length is preferred for higher detection sensitivity.

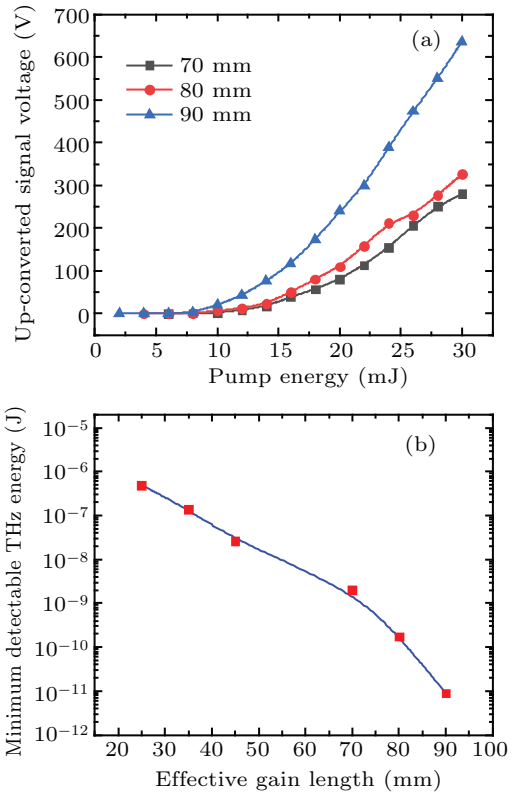


Fig. 5. (a) Measured voltage of the up-converted signal as a function of pump energy at different effective gain lengths. (b) The minimum detectable THz wave energy as a function of effective gain length.

Finally, the frequency detection range of the parametric up-conversion detector was studied. Figure 6 shows the measured spectra of the up-converted signals at different wavelengths from 1068.70 nm to 1071.11 nm, corresponding to the THz frequency range of 0.9 THz–1.83 THz. When the input THz frequency was 1.83 THz, the minimum detectable energy was 100 pJ, which was still much higher than that of the Golay cell. Then, the up-converted signal was hardly observed while

the input THz frequency was larger than 1.83 THz or smaller than 0.9 THz. This can be attributed that the THz wave generated from ips-TPG has relatively large divergence angle and different emission direction for each frequency, which cannot be well focused into CLN1 crystal beyond the range of 0.9 THz–1.83 THz using our current focusing setup. The focusing method should be furtherly optimized to improve the interact effect between THz wave and pump beam.

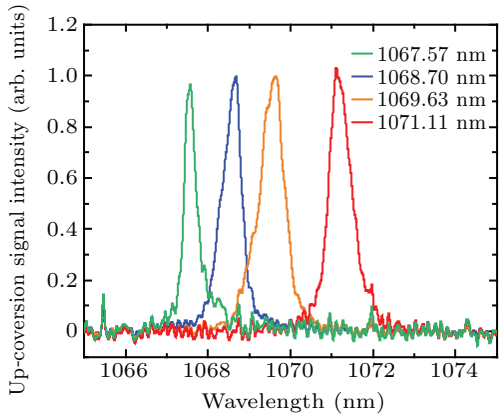


Fig. 6. The frequency detection range of parametric up-conversion detection: 0.90 THz–1.83 THz.

4. Conclusion

In this work, a high-sensitive THz parametric up-conversion detector pumped by ns 1064-nm Nd:YAG laser was investigated. The detection system operated at room temperature realized a high sensitivity detection of 9 pJ and a dynamic range of 54 dB, which was three orders of magnitude higher than that of conventional Golay cell. And the frequency range of 0.90 THz–1.83 THz was realized, with the lowest sensitivity of 100 pJ at the whole detectable range. Moreover, the effects of pump energy and effective gain length on the detection sensitivity of THz parametric up-conversion detection were investigated. The results showed that higher pump energy and longer effective gain length are beneficial to improving the sensitivity of parametric up-conversion detector. It is expected that such ns laser-pumped THz detector with high sensitivity can provide good advantages and enlarge applicable scope of THz wave.

Acknowledgements

Project supported by the National Natural Science Foundation of China (Grant Nos. U1837202, 61775160, 61771332, 62011540006, and 62175182).

The authors appreciate the fruitful discussion with Prof. Kai Zhong, Dr. Longhuang Tang and Hongzhan Qiao of Institute of Laser and Optoelectronics, School of Precision Instruments and Optoelectronics Engineering, Tianjin University.

References

[1] Elayan H, Amin O, Shubair R M, Yevgeni Koucheryavy Y 2018 *International Conference on Advanced Communication Technologies and Networking*, April 2–4, 2018, Marrakech, Morocco, p. 1

[2] Taylor Z D, Singh R S, Culjat M O and Culjat J 2008 *Opt. Lett.* **33** 1258

[3] Davies A G, Burnett A D, Fan W H, Linfield E H and Cunningham J E 2008 *Mater. Today* **11** 18

[4] Pawar A Y, Sonawane D D, Erande K B and Derle D V 2013 *Drug Invent. Today* **5** 157

[5] Wu Q and Zhang X C 1995 *Appl. Phys. Lett.* **67** 3523

[6] Wu B, Cao L, Zhang Z, Fu Q and Xiong Y Q 2018 *IEEE Trans. Terahertz Sci. Technol.* **8** 305

[7] Kampfrath T, Nötzold J and Wolf M 2007 *Appl. Phys. Lett.* **90** 231113

[8] Babin A A, Petryakov V N and Freidman G I 1983 *Sov. J. Quantum Electron.* **13** 958

[9] Kong W P, Yan Q, Li Z Y, Zou M R, Zhou X and Qin Y 2020 *IEEE Trans. Terahertz Sci. Technol.* **11** 389

[10] Mine S, Kawase K and Murate K 2021 *Opt. Lett.* **46** 2618

[11] Shi J L, Xu J, Luo N N, Wang Q, Zhang Y B, Zhang W W and He X D 2019 *Acta Phys. Sin.* **68** 044201 (in Chinese)

[12] Faris G W, Jusinski L E and Hickman A P 1993 *J. Opt. Soc. Am. B* **10** 587

[13] Faris G W, Dyer M J and Hickman A P 1992 *Opt. Lett.* **17** 1049

[14] Sentrayan K and Kushawaha V 1993 *J. Phys. D: Appl. Phys.* **26** 1554

[15] Minamide H, Hayashi S, Nawata K, Taira T, Shikata J I and Kawase K 2014 *J. Infrared, Millimeter, Terahertz Waves* **35** 25

[16] Hayashi S I, Nawata K, Taira T, Shikata J I, Kawase K and Minamide H 2014 *Sci. Rep.* **4** 1

[17] Kato M, Tripathi S R, Murate K, Imayama K and Kawase K 2016 *Opt. Express* **24** 6425

[18] Sakai H, Kawase K and Murate K 2020 *Opt. Lett.* **45** 3905

[19] Takida Y, Nawata K, Suzuki S, Asada M and Minamide H 2017 *Opt. Express* **25** 5389

[20] Takida Y, Nawata K, Suzuki S, Asada M and Minamide H 2017 *AIP Adv.* **7** 035020

[21] Yan C, Wang Y Y, Xu D G, Xu W T, Liu P X, Yan D X, Duan P, Zhong K, Shi W and Yao J Q 2016 *Appl. Phys. Lett.* **108** 011107

[22] Wang Y Y, Tang L H, Xu D G, Yan C, He Y X, Shi J, Yan D X, Liu H X, Nie M T, Feng J C and Yao J Q 2017 *Opt. Express* **25** 8926

[23] Tang L H, Xu D G, Wang Y Y, Yan C, He Y X, Li J N, Zhong K and Yao J Q 2019 *Opt. Express* **27** 22808

[24] Guo R X, Ohno S, Minamide H, Ikari T and Ito H 2008 *Appl. Phys. Lett.* **93** 021106

[25] Guo R X, Ikar T, Zhang J, Minamide H and Ito H 2010 *Opt. Lett.* **18** 16430

[26] Shikata J I, Kawase K, Karino K I, Taniuchi T and Ito H 2000 *IEEE Trans. Microwave Theory Tech.* **48** 653